

# Structural Features of Aliphatic *N*-Nitrosamines of 7-Azabicyclo[2.2.1]heptanes That Facilitate N–NO Bond Cleavage

Tomohiko Ohwada,<sup>\*,†</sup> Motoko Miura,<sup>‡</sup> Haruko Tanaka,<sup>‡</sup> Shigeru Sakamoto,<sup>§</sup> Kentaro Yamaguchi,<sup>§</sup> Hirotaka Ikeda,<sup>||</sup> and Satoshi Inagaki<sup>||</sup>

Contribution from the Graduate School of Pharmaceutical Sciences, The University of Tokyo, 7-3-1 Hongo, Bunkyo-ku, Tokyo, 113-0033, Japan, Faculty of Pharmaceutical Sciences, Nagoya City University, Tanabe-dori, Mizuho-ku, Nagoya, 467-8603, Japan, Chemical Analysis Center, Chiba University, Yayoi-cho, Inage-ku, Chiba 263-8522, Japan, and Department of Chemistry, Faculty of Engineering, Gifu University, Yanagido, Gifu 501-1193, Japan

Received April 9, 2001

**Abstract:** *N*-Nitrosamines can be considered as potential nitric oxide (NO)/nitrosonium ion (NO<sup>+</sup>) donors. However, the relation of the structures of *N*-nitrosamines, in particular of aliphatic *N*-nitrosamines, to the characteristics of release of NO or NO<sup>+</sup> remains unclear. Here we show that aliphatic *N*-nitrosamines of 7-azabicyclo[2.2.1]heptanes can undergo heterolytic N–NO bond cleavage. On the basis of the observation of reduced rotational barriers of the N–NO bonds in solution and nitrogen-pyramidal structures of the *N*-nitroso group in the solid state, we postulate that N–NO bond cleavage of *N*-nitrosamines is enhanced by a reduction of the resonance in the N–NO group. Computational studies suggest that these structural features of the *N*-nitrosamines of 7-azabicyclo[2.2.1]heptane are derived from angle strain imposed on the CNC angles.

## Introduction

The identification of the physiological activity of nitric oxide (NO) has generated much interest in the chemistry of NO-related bonding, both as regulation of many important physiological functions in living bodies and as possible pharmaceutical delivery systems.<sup>1</sup> Two possible modes of cleavage of the N–NO bond of *N*-nitrosamines, that is, homolytic and heterolytic cleavages are well recognized (Figure 1).<sup>2,3</sup> Aromatic *N*-nitrosamines<sup>2</sup> and aromatic *N*-nitrosoureas<sup>3</sup> were demonstrated to undergo homolytic cleavage of the N–NO bond to give NO.<sup>1</sup> Aromatic *N*-nitrosoureas and *N*-nitrososulfonamides were also shown to be heterolytically cleaved to give nitrosonium ion (NO<sup>+</sup>) in solution.<sup>3</sup> Thus, some aromatic *N*-nitroso compounds can act as donors of NO or NO<sup>+</sup>. On the other hand, aliphatic *N*-nitrosoureas do not release NO,<sup>3</sup> and there has been no report of aliphatic *N*-nitrosamines that readily undergo N–NO bond cleavage.

Available donors of NO include *S*-nitroso compounds<sup>4</sup> and anionic diazeniumdiolates (NONOates),<sup>5</sup> both of which are water-soluble (Figure 2). The release of NO by the latter donors is rapid under physiological conditions (pH 7.4), that is, the

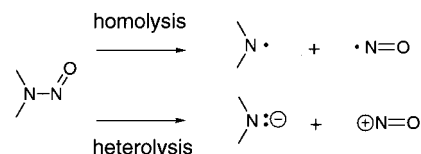


**Figure 1.** Two possible modes of N–NO bond cleavage of *N*-nitrosamines.

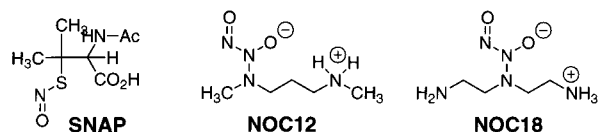


**Figure 2.** Available donors of NO.

half-life typically ranges from 2 to 30 min.<sup>4,5</sup> In organisms, NO has many potent biological activities and is characteristically present at extremely low levels.<sup>3,6,f</sup> Local high concentrations of NO are toxic to living tissues.<sup>3</sup> For medicinal purposes, it is desirable to find NO-donating compounds with well-controlled release.

Amine derivatives of 7-azabicyclo[2.2.1]heptane (7-azanorbornane) are known to have high nitrogen inversion barriers,

(4) (a) *S*-Nitroso-*N*-acetyl-DL-penicillamine (SNAP): Field, L.; Dilts, R. V.; Ravichandran, R.; Lenhart, P. G.; Carnahan, G. E. *J. Chem. Soc., Chem. Commun.* **1978**, 249–250. (b) Williams, D. L. H. *Acc. Chem. Res.* **1999**, 32, 869–876. (c) Martberger, M. D.; Houk, K. N.; Powell, S. C.; Mannion, J. D.; Lo, K. Y.; Stamler, J. S.; Toone, E. J. *J. Am. Chem. Soc.* **2000**, 122, 5889–5890.

(5) NOC12 (*N*-ethyl-2-(1-ethyl-2-hydroxy-2-nitrosohydrazino)ethanamine); NOC18 (2,2'-(hydroxynitrosohydrazino)bisethanamine), see Maragos, C. M.; Morley, D.; Wink, D. A.; Dunams, T. M.; Saavedra, J. E.; Hoffman, A.; Bove, A. A.; Isaac, L.; Hrabie, J. A.; Keefer, L. K. *J. Med. Chem.* **1991**, 34, 3242–3247. Hrabie, J. A.; Klöse, J. R.; Wink, D. A.; Keefer, L. K. *J. Org. Chem.* **1993**, 58, 1472–1476. Saavedra, J. E.; Shami, P. J.; Wang, L. Y.; Davies, K. M.; Booth, M. N.; Citro, M. L.; Keefer, L. K. *J. Med. Chem.* **2000**, 43, 261–269. Davies, K. M.; Wink, D. A.; Saavedra, J. E.; Keefer, L. K. *J. Am. Chem. Soc.* **2001**, 123, 5473–5481.

<sup>†</sup> The University of Tokyo.

<sup>‡</sup> Nagoya City University.

<sup>§</sup> Chiba University.

<sup>||</sup> Gifu University.

(1) (a) Murad, F. *Angew. Chem., Int. Ed.* **1999**, 38, 1856–1868 and references therein. (b) Ignarro, L. J. *Angew. Chem., Int. Ed.* **1999**, 38, 1882–1892 and references therein. (c) Furchgott, R. F. *Angew. Chem., Int. Ed.* **1999**, 38, 1870–1880 and references therein. (d) Pfeiffer, S.; Mayer, B.; Hemmen, B. *Angew. Chem., Int. Ed.* **1999**, 38, 1714–1731, and references therein. (e) Stamler, J. S.; Jaraki, O.; Osborne, J.; Simon, D. I.; Keaney, J.; Vita, J.; Singel, D.; Valeri, C. R.; Loscalzo, J. *Proc. Natl. Acad. Sci. U.S.A.* **1992**, 89, 7674–7677. (f) Stamler, J. S.; Singel, D. J.; Loscalzo, J. *Science* **1992**, 258, 1898–1902.

(2) (a) Tanno, M.; Sueyoshi, S.; Miyata, N.; Nakagawa, S. *Chem. Pharm. Bull.* **1996**, 44, 1849–1852. (b) Tanno, M.; Sueyoshi, S.; Miyata, N.; Umehara, K. *Chem. Pharm. Bull.* **1997**, 45, 595–598.

(3) Cheng, J.-P.; Xian, M.; Wang, K.; Zhu, X.; Yin, Z.; Wang, P. G. *J. Am. Chem. Soc.* **1998**, 120, 10266–10267.

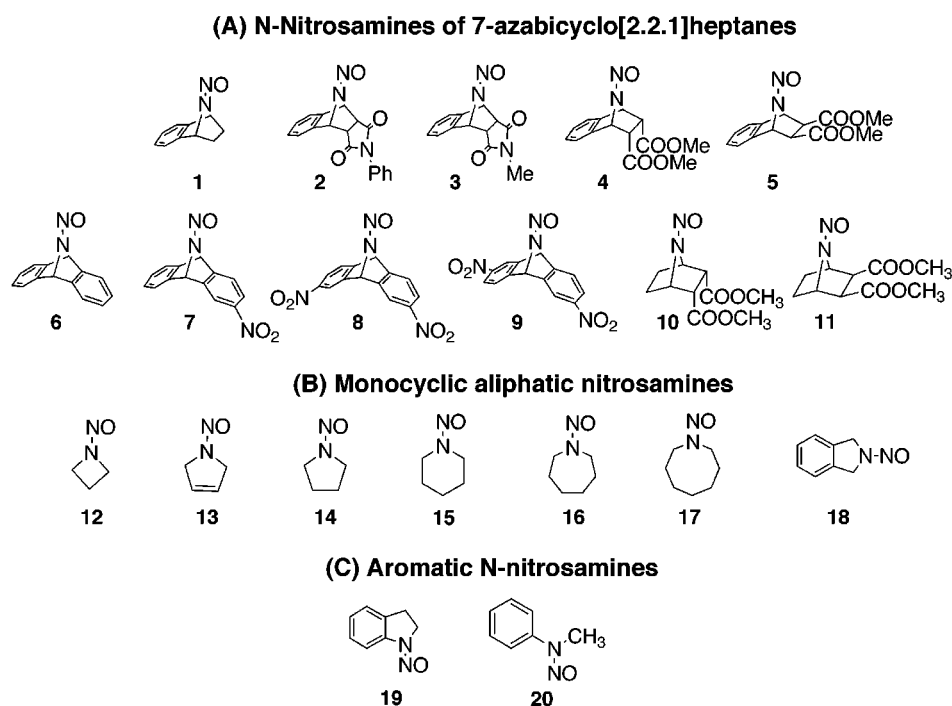


**Figure 3.** N-Nitrosamines in this study.

close to those in aziridines.<sup>6</sup> Thus, we focused on *N*-nitroso derivatives of 7-azabicyclo[2.2.1]heptanes (**1–11**) as candidate donors of NO and related species (Figure 3). A range of monocyclic aliphatic *N*-nitrosamines (**12–18**) was prepared in order to assess the effect of the additional bridging (Figure 3B). Structurally related aromatic *N*-nitrosamines (**19** and **20**) were also prepared as reference compounds (Figure 3C). In this contribution, we show that aliphatic *N*-nitrosamines of 7-azabicyclo[2.2.1]heptanes can undergo readily heterolytic N–NO bond cleavage.<sup>7</sup> To understand the structural origins of the facile N–NO bond cleavage of certain bicyclic *N*-nitrosamines, we evaluated the rotational barriers of the N–NO bonds by using dynamic NMR spectroscopy in solution and assessed the nitrogen-pyramidal character of the *N*-nitroso group in 7-azabicyclo[2.2.1]heptane derivatives. Computational evaluation of the structures, rotational barriers, and bond dissociation energies of the N–NO bond, and analysis of the electronic structure of the N–NO bonds on the basis of the bond model method,<sup>8</sup> highlighted the significance of angle strain imposed on the CNC angle in promoting N–NO bond cleavage.

## Results and Discussion

**Griess Assay Results, Reflecting the Ease of N–NO Bond Cleavage of the *N*-Nitrosamines.** Release of NO or NO<sup>+</sup> from *N*-nitrosamines in solution (Figure 1) can be detected with the Griess method.<sup>9</sup> NO reacts with oxygen in water to generate nitrate ion which yields NO<sup>+</sup> in an acidic medium.<sup>1,9</sup> The visible absorption at 595 nm of the resultant red dye formed upon diazo coupling of the Griess reagents, allows evaluation of the amount of NO or NO<sup>+</sup> formed by cleavage of the N–NO bonds of

*N*-nitrosamines. After 5 h at 37 °C, the absorbance at 595 nm was measured (Figure 4).

Authentic NO donors, *N*-ethyl-2-(1-ethyl-2-hydroxy-2-nitrosohydrazino)ethanamine (NOC12), 2,2'-(hydroxynitrosohydrazino)bisethanamine (NOC18), and *S*-nitroso-*N*-acetyl-DL-penicillamine (SNAP) (Figure 2) were also studied as positive controls.<sup>4,5</sup> The absorption increased dose-dependently except in the cases of compounds **6**, **7**, **8**, and **9**, which did not dissolve completely in the Griess reagents at 0.5 and 0.25 mM. Although the monocyclic aliphatic *N*-nitrosamines with four (**12**)-, five (**13**, **14**, and **18**)-, six (**15**)-, seven (**16**)-, and eight (**17**)-membered rings were practically negative in the Griess assay, the *N*-nitroso derivatives (**2–9**) of the 7-azabicyclo[2.2.1]heptane motif were positive (weakly positive in the cases of **1**, **10**, and **11**). Some of these bicyclic derivatives were better NO donors than the aromatic *N*-nitrosamines (**19** and **20**) and authentic NO donors (NOC12, NOC18, and SNAP) (Figure 4). In the Griess assay, which reflects the ease of N–NO bond cleavage, electron-withdrawing groups, such as an aromatic nitro group (**7–9**), ester groups (**4** and **5**), and the *N*-phenylimido group (**2** and **3**), enhanced N–NO bond cleavage of the *N*-nitroso derivatives of the 7-azabicyclo[2.2.1]heptanes as compared with the unsubstituted derivatives (**1** and **6**) (in Figure 4: **2**, **3**, **4**, **5** > **1**; **7**, **8**, **9** > **6**).

Time-dependent formation of the dye in the Griess assay reflects the profile of the release of NO or NO<sup>+</sup> species from the relevant nitrosamines (Figure 5). The absorption of the produced dye was measured at 1-h intervals until 6 h in the Griess assay at 37 °C.

The *N*-nitroso derivatives (**2–8**) of 7-azabicyclo[2.2.1]heptane, aromatic *N*-nitrosamines (**19** and **20**), and SNAP increased the concentration of the formed dye time-dependently (in Figure 5, **2**, **7**, **8**, and **19** are shown), while the authentic NO donors, NOC12 and NOC18, that is, NONOate-type donors, showed rapid formation of the dye, and the concentration of the formed dye did not change significantly during 6 h.

(6) (a) Lehn, J. M. *Fortshr. Chem. Forsch.* **1970**, *15*, 311–377. (b) Lambert, J. B.; Oliver, W. L., Jr.; Packard, B. S. *J. Am. Chem. Soc.* **1971**, *93*, 933. (c) Nelsen, S. F.; Ippoliti, J. T.; Frigo, T. B.; Petillo, P. A. *J. Am. Chem. Soc.* **1989**, *111*, 1776–1781. (d) Belostotskii, A. M.; Gottlieb, H. E.; Hassner, A. *J. Am. Chem. Soc.* **1996**, *118*, 7783–7789.

(7) A part of the work was communicated in Miura, K.; Sakamoto, S.; Yamaguchi, K.; Ohwada, T. *Tetrahedron Lett.* **2000**, *41*, 3637–3641.

(8) (a) Iwase, K.; Inagaki, S. *Bull. Chem. Soc. Jpn.* **1996**, *69*, 2781–2789. (b) Inagaki, S.; Ikeda, H. *J. Org. Chem.* **1998**, *63*, 7820–7824 and references therein.

(9) Green, L. C.; Wagner, D. A.; Glogowski, J.; Skipper, P. L.; Wishnok, J. S.; Tannenbaum, S. T. *Anal. Chem.* **1982**, *126*, 131–138.

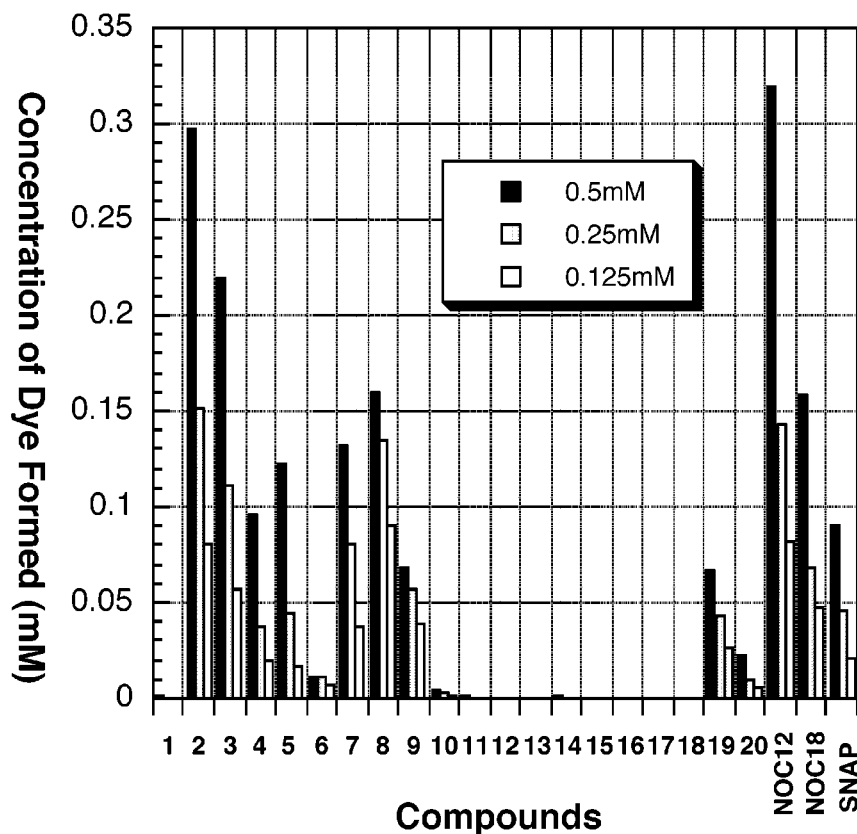


**Figure 4.** Griess assay results, reflecting the ease of N–NO bond cleavage of the *N*-nitrosamines, after 5 h at 37 °C.

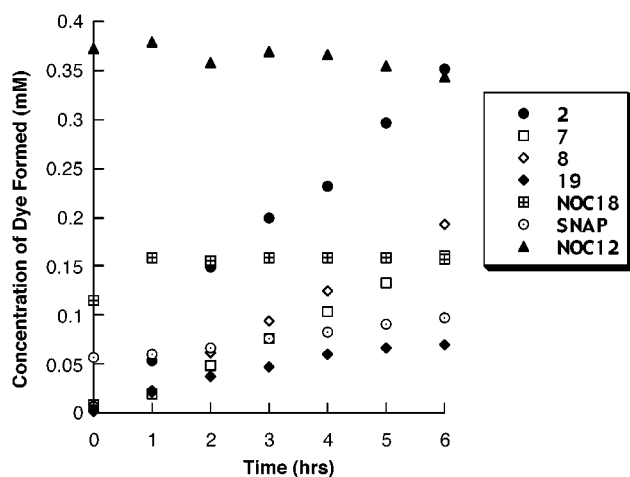


**Figure 5.** Time-dependent formation of dye. Initial concentration of compounds is 0.5 mM.

Under the original Griess assay conditions, which involve phosphoric acid,<sup>9</sup> the solution is acidic, that is, pH 2.1. The pH value of the medium was adjusted to 2.5 or 3.4 by addition of solid sodium carbonate, and the Griess assay was carried out at each pH (Supporting Information, Figure S1). While NOC12 is insensitive to the pH of the medium, giving a rapid and steady formation of the dye (these data also supported the facile Griess reaction at each pH), the imide **2**, **19**, and SNAP showed acidity-dependent dye formation. Therefore, acidic conditions enhance N–NO bond cleavage of the bicyclic *N*-nitrosamines.

**Detection of Released Isoform of NO from Bicyclic *N*-Nitrosamines.** Detection of the nitrogen species released from the bicyclic *N*-nitrosamines was carried out with a spin-trapping reagent, the potassium salt of 2-(4-carboxyphenyl)-4,4,5,5-tetramethylimidazole-1-oxyl-3-oxide (carboxy-PTIO), which

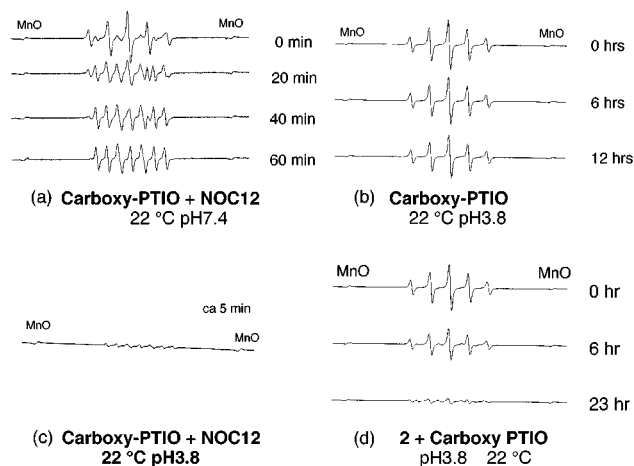


**Figure 6.** Detection of nitrogen species released from *N*-nitrosamines.

reacts with  $\cdot\text{NO}$  to give 2-(4-carboxyphenyl)-4,4,5,5-tetramethylimidazole-1-oxyl (carboxy-PTI) and  $\cdot\text{NO}_2$ .<sup>10</sup> The spectral change of carboxy-PTIO to carboxy-PTI was utilized for detection of NO by ESR spectroscopy (Figure 6a).

At physiological pH (7.4, in PBS buffer), no significant change of the spectrum of carboxy-PTIO was seen in the presence of the nitrosamine **2** at 22 °C (data not shown). At pH 3.8 (in a mixture of PBS buffer and aqueous HCl), the ESR spectra of carboxy-PTIO slowly changed, and the intensity of the signals was significantly reduced after 24 h (Figure 6d). In the acidic medium (pH 3.8), carboxy-PTIO is stable for at least 12 h when an NO-donating agent is absent, as judged from the shapes and magnitude of the ESR signals (Figure 6b). Addition

(10) Akaike, T.; Yoshida, M.; Miyamoto, Y.; Sato, K.; Kohno, M.; Sasamoto, K.; Miyazaki, K.; Ueda, S.; Maeda, H. *Biochemistry* **1993**, *32*, 827–832.

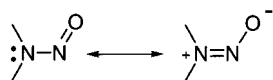


**Figure 7.** Resonance model of planar nitrogen of *N*-nitrosamines.

of NOC12, an authentic NO donor, to the aqueous solution of carboxy-PTIO caused the signals of carboxy-PTIO to disappear immediately at pH 3.8 (Figure 6c). This indicates that the resultant carboxy-PTI was unstable in acidic media. The reduction of the signals of carboxy-PTIO in the presence of the nitrosamine **2** at 22 °C at pH 3.8 (Figure 6d) suggested that NO was formed from the nitrosamine **2**, and the reaction was very slow. A similar slow change of the ESR spectra of carboxy-PTIO in the presence of another bicyclic nitrosamine **7** or the aromatic *N*-nitrosamine **19** was also observed (Supporting Information, Figure S2 a and b). These slow changes of the ESR spectra exclude rapid formation of NO from these nitrosamines even in an acidic medium. Therefore, we can reasonably interpret the observed Griess reaction in terms of the formation of NO<sup>+</sup> ion upon acid-catalyzed heterolytic cleavage of the N–NO bonds of the bicyclic *N*-nitrosamines.

**Rotational Barriers of the N–NO Bonds.** *N*-Nitroso compounds generally take planar structures, because the rotational barriers of the N–NO bond<sup>11–13</sup> are of similar magnitude to those of amides.<sup>14,15</sup> This can be understood in terms of the resonance structures (Figure 7), which represent the partial double bond character of the N–N(O) bond, in a manner similar to the N–C(O) bond in amides.

Rotational barriers in solution, the free energy of activation ( $\Delta G_c^\ddagger$ ), of the *N*-nitrosamines can be evaluated by variable-temperature <sup>1</sup>H NMR spectroscopy (Table 1).<sup>15</sup> The rotational barriers are consistent among several solvents of different polarity (Table 1). The values ( $\Delta G_c^\ddagger$ ) of the *N*-nitroso derivatives of 7-azabicyclo[2.2.1]heptanes (**1–11**) are apparently smaller than those of the monocyclic five-membered *N*-nitrosamines (**13** and **14**). This result suggests a reduction of the resonance contribution of the N–NO bond, as depicted in Figure 7 in the *N*-nitroso derivatives of the 7-azabicyclo[2.2.1]heptane motif. The rotational barriers of the isoindoline **18** and other monocyclic *N*-nitrosamines (**12** and **15–17**) are estimated to be more than 20–21 kcal/mol. The rotational barrier of *N*-nitrosoazetidine **12** is comparable to those of the five-membered ring

**Table 1.** Rotational Barriers of *N*-Nitrosamines

cmpd	solvent <sup>a</sup>	$T_c$ (°C) <sup>b</sup>	$\Delta G_c^\ddagger$ (kcal/mol) <sup>c</sup>	cmpd	solvent <sup>a</sup>	$T_c$ (°C) <sup>b</sup>	$\Delta G_c^\ddagger$ (kcal/mol) <sup>c</sup>
<b>1</b>	A	71.2	16.6	<b>10</b>	B	37.9	14.6
<b>2</b>	B	36.9	15.1	<b>11</b>	A	61.0	16.7
	C	51.9 <sup>d</sup>	15.5	<b>12</b>	B	65.7	17.2
<b>3</b>	B	43.6	15.1	<b>13</b>	C	158.0	20.1
<b>4</b>	B	53.6	15.8	<b>14</b>	C	157.2	21.5
	C	63.9 <sup>d</sup>	16.1	<b>15</b>	C	>170.1 <sup>e</sup>	>20.6
<b>5</b>	A	63.9	16.7	<b>16</b>	C	>170.1 <sup>e</sup>	>21.1
<b>6</b>	B	52.7	16.0	<b>17</b>	C	>170.0 <sup>e</sup>	>20.6
<b>7</b>	B	47.2	15.4	<b>18</b>	C	>170.1 <sup>e</sup>	>20.8
<b>8</b>	B	36.1	14.6	<b>19</b>	C	>170.4 <sup>e</sup>	>20.6
<b>9</b>	A	37.2	14.7				

<sup>a</sup> A: CD<sub>2</sub>ClCD<sub>2</sub>Cl; B: CDCl<sub>3</sub>; C: C<sub>6</sub>D<sub>5</sub>NO<sub>2</sub>. <sup>b</sup> Errors: ±1.0 °C. Temperatures were calibrated by means of a standard method.<sup>24</sup> <sup>c</sup> Rotational barriers ( $\Delta G_c^\ddagger$ ) were obtained on the basis of the difference in chemical shifts of the two bridgehead proton signals and the coalescence temperature in proton NMR spectroscopy. Errors: ±0.3 kcal/mol. <sup>d</sup> Based on the coalescence of aromatic protons. <sup>e</sup> The maximum measurable with the apparatus.

systems (**13** and **14**), the value being consistent with the previous result (20.5 kcal/mol).<sup>12</sup> The dibenzo derivatives (**6–9**) also have small rotational barriers (Table 1). The present results are consistent with the idea that the aliphatic *N*-nitrosamines with a low rotational barrier of the N–NO bond will be positive in the Griess assay (weakly positive in the cases of **1**, **10**, and **11**), that is, reduction of *N*-nitroso resonance (Figure 7) facilitates N–NO bond cleavage.

**Crystallographic Studies of Bicyclic Nitrosamines.** To examine the structural features of the relevant *N*-nitrosamines we carried out crystallographic studies of single crystals of some of them. Planarity of nitrogen can be represented in terms of the angle parameter  $\theta$  (summation of the three angles around the nitrogen atom; for planar nitrogen,  $\theta = 360.0^\circ$ ) and also in terms of the hinge angle  $\alpha$  (Figure 8; if the nitrogen is planar,  $\alpha = 180.0^\circ$ ).

A single-crystal structure determination of monocyclic *N*-nitrosopyrroline (**13**) (at 113 K (–160 °C)) revealed a planar nitrogen atom of the pyrroline ring ( $\theta = 359.9(2)^\circ$ ,  $\alpha = 180.0^\circ$ ) (Table 2),<sup>16</sup> which is consistent with the resonance model (Figure 7). The bond lengths of the N–N and N–O bonds of **13** are 1.311(3) and 1.251(3) Å, respectively, and the angle  $\angle$ NNO is 113.1(2)°. The bond angles of the N–NO bond, two  $\angle$ CNN angles are 119.9(2)° and 126.1(2)°, respectively. The crystal structure of *N*-nitrosoisoindoline (**19**) (at 296 K (23 °C)) also revealed a typical planar structure of the *N*-nitroso group (Table 2) ( $\theta = 359.9(3)^\circ$ ,  $\alpha = 180.0^\circ$ ).<sup>17</sup>

On the other hand, a single-crystal structure of bicyclic *N*-nitrosobenzo-7-azabicyclo[2.2.1]heptane **2** revealed nitrogen pyramidalization (Figure 8 and Table 2).<sup>18</sup> In the case of **2**, two kinds of molecules are found in a unit cell; these are considered to be isomers arising from the rotations about the N–NO bond

(16) **Crystallographic data for *N*-nitrosoisopyrrolidine **13**:** C<sub>4</sub>H<sub>6</sub>N<sub>2</sub>O,  $M_r = 98.10$ , 0.45 mm × 0.25 mm × 0.13 mm, orthorhombic *Pna*2<sub>1</sub>,  $a = 12.74(2)$  Å,  $b = 5.851(8)$  Å,  $c = 6.372(7)$  Å,  $V = 474(1)$  Å<sup>3</sup>,  $Z = 4$ ,  $D_x = 1.372$  g/cm<sup>3</sup>,  $2\theta_{\max} = 55.1^\circ$ ,  $T = 113$  K,  $\mu(\text{Mo K}\alpha) = 1.02$  cm<sup>–1</sup>,  $F_{000} = 208$ , Rigaku RAXIS-II Imaging Plate diffractometer,  $\omega$  scans, 562 refs measured, 554 unique, 515 with  $I > 3.0\sigma(I)$ , 65 variables,  $R = 0.065$ ,  $R_w = 0.077$ ,  $S = 2.31$ ,  $(\Delta/\sigma)_{\max} = 2.709$ ,  $\rho_{\max} = 0.30$  eÅ<sup>–3</sup>,  $\Delta\rho_{\min} = -0.33$  eÅ<sup>–3</sup>.

(17) **Crystallographic data for *N*-nitrosoindoline **19**:** C<sub>8</sub>H<sub>8</sub>N<sub>2</sub>O,  $M_r = 148.16$ , 0.40 mm × 0.40 mm × 0.20 mm, monoclinic *P2*<sub>1</sub>/*c*,  $a = 8.6863(8)$  Å,  $b = 10.8875(12)$  Å,  $c = 8.4161(9)$  Å,  $\beta = 112.390(3)^\circ$ ,  $V = 735.93(12)$  Å<sup>3</sup>,  $Z = 4$ ,  $D_x = 1.337$  g/cm<sup>3</sup>,  $2\theta_{\max} = 57.0^\circ$ ,  $T = 296$  K,  $\mu(\text{Mo K}\alpha) = 0.92$  cm<sup>–1</sup>,  $F_{000} = 312$ , Bruker SMART CCD diffractometer,  $\omega$  scans, 6252 refs measured, 1973 unique, 873 with  $I > 3.0\sigma(I)$ , 101 variables,  $R = 0.055$ ,  $R_w = 0.073$ ,  $S = 1.42$ ,  $(\Delta/\sigma)_{\max} = 0.01$ ,  $\rho_{\max} = 0.17$  eÅ<sup>–3</sup>,  $\Delta\rho_{\min} = -0.22$  eÅ<sup>–3</sup>.

(11) (a) Loeppky, R. N.; Michejda, C. J. *N-Nitrosamines and Related N-Nitroso Compounds*; ACS Symposium Series 553; American Chemical Society: Washington, DC, 1994. (b) Oh, S. M. N. Y. F.; Williams, D. L. *J. Chem. Soc., Perkin Trans. 2* **1989**, 755–758. (c) Castro, A.; Leis, J. R.; Pena, M. E. *J. Chem. Soc., Perkin Trans 2* **1989**, 1861–1866. (d) Galtress, C. L.; Morrow, P. R.; Nag, S.; Smalley, T. L.; Tschantz, M. F.; Vaughn, J. S.; Wichems, D. N.; Ziglar, S. K.; Fishbein, J. C. *J. Am. Chem. Soc.* **1992**, *114* 1406–1411. (e) Santala, T.; Fishbein, J. C. *J. Am. Chem. Soc.* **1992**, *114*, 8852–8857.

(12) Cooney, J. D.; Brownstein, S. K.; Apsimon, J. W. *Can. J. Chem.* **1974**, *52*, 3028–3036. High rotational barriers of the N–NO bond (<23 kcal/mol) of different bicyclic *N*-nitrosamines were also reported.

(13) (a) Harris, R. K.; Pryce-Jones, T.; Swinbourne, F. J. *J. Chem. Soc., Perkin Trans. 2* **1980**, 476–482. (b) *N*-Nitrosoindoline (**15**) and *N*-methyl-*N*-phenylnitrosamine (**16**) exist as a single conformational isomer. See: Looney, C. E.; Phillips, W. D.; Reilly, E. L. *J. Am. Chem. Soc.* **1957**, *79*, 6136–6142. The rotational barrier of an aromatic *N*-nitrosamine, *N*-nitrosodiphenylamine, was reported to be 19.1 kcal/mol by Forlani et al. Forlani, L.; Lunazzi, L.; Macciantelli, D.; Minguzzi, B. *Tetrahedron Lett.* **1979**, 1451–1452.

(14) (a) Gropen, O.; Skancke, P. N. *Acta Chem. Scand.* **1971**, *25*, 1241–1249. (b) Gdaniec, M.; Milewska, M. J.; Polonski, T. *J. Org. Chem.* **1995**, *60*, 7411–7418.

(15) (a) Mannschreck, A.; Münsch, H.; Mattheus, A. *Angew. Chem., Int. Ed. Engl.* **1966**, *5*, 728. (b) Mannschreck, A.; Münsch, H. *Angew. Chem., Int. Ed. Engl.* **1967**, *6*, 984–985. (c) Oki, M. *Applications of Dynamic NMR Spectroscopy to Organic Chemistry*; VCH Publishers: Deerfield, USA, 1985; Vol. 4.

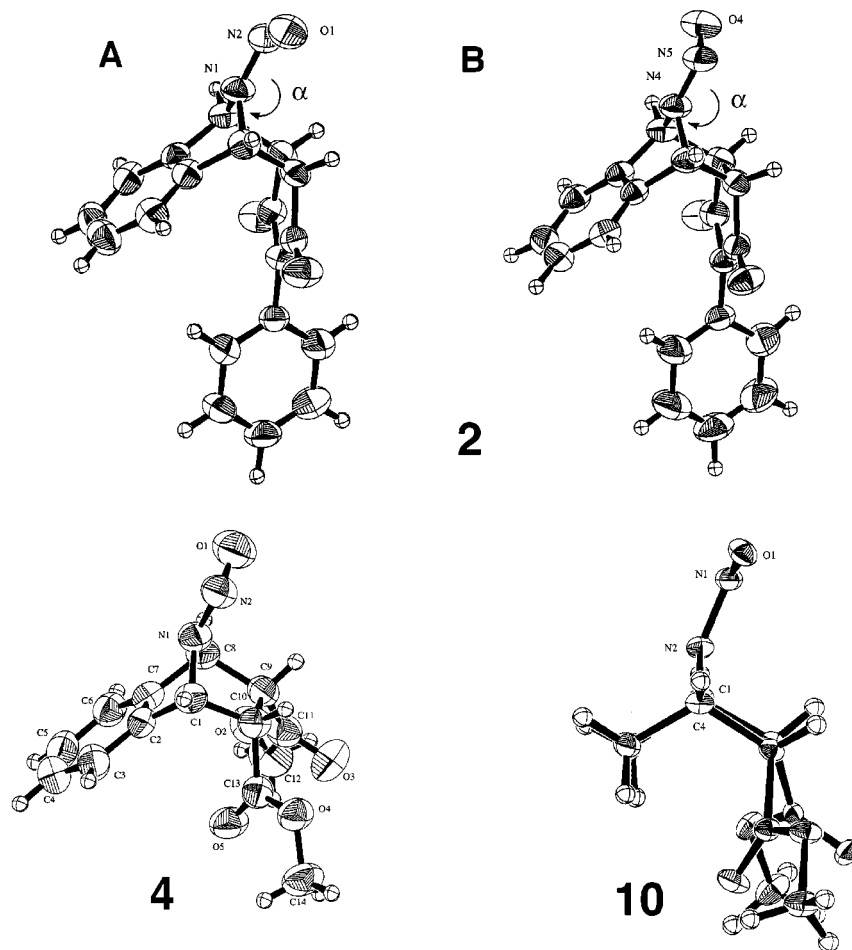


**Figure 8.** ORTEP diagrams of nitrogen-pyramidal *N*-nitrosamines, showing 50% probability displacement ellipsoids (**2** and **4**: at 23 °C; **10**: at -160 °C).

**Table 2.** Selected Geometrical Parameters of Single Crystal Structures of *N*-Nitrosamines

cmpd	N–N (Å)	N–O (Å)	∠NNO (deg)	∠CNN (deg)	∠CNC (deg)	θ(deg) <sup>a</sup>	α <sup>b</sup>
<b>2</b> <sup>c,d</sup>	1.311(4)	1.237(4)	113.5(3)	130.0(3), 122.5(3)	98.7(2)	351.2(3)	155.2
	1.313(4)	1.253(5)	112.8(4)	129.0(3), 122.5(3)	99.1(3)	350.6(3)	154.2
<b>4</b> <sup>d</sup>	1.314(5)	1.226(5)	112.7(4)	129.3(3), 121.3(3)	99.2(3)	349.8(3)	153.1
<b>10</b> <sup>e</sup>	1.310(3)	1.247(2)	114.7(2)	128.6(2), 124.5(2)	99.4(2)	352.5(2)	157.1
<b>13</b> <sup>e</sup>	1.311(3)	1.251(3)	113.1(2)	126.1(2), 119.9(2)	113.9(2)	359.9(2)	180.0
<b>19</b> <sup>d</sup>	1.294(3)	1.252(4)	113.8(3)	125.4(3), 122.8(3)	111.7(2)	359.9(3)	180.0

<sup>a</sup> Angle  $\theta$  is the sum of the three valence angles around the amine nitrogen atom. <sup>b</sup> The angle  $\alpha$  is the hinge angle. <sup>c</sup> Two kinds of molecule are involved in a unit cell <sup>d</sup> At 23 °C. <sup>e</sup> At -160 °C.

and the imido N–Ph bond. The angles  $\theta$  were 351.2(3)° and 350.6(3)° in the case of the two molecules of **2**, and the hinge angles  $\alpha$  are 155.2° and 154.2°, respectively. Similar nitrogen pyramidalization was found in the single-crystal structures of the bicyclic *N*-nitrosamines **4** (at 23 °C) and **10** (at -160 °C) (Table 2 and Figure 8).<sup>19,20</sup> This nitrogen pyramidalization might contribute to the reduction of resonance in the N–NO group in solution.

**Ab initio Calculations of Bicyclic and Monocyclic *N*-Nitrosamines.** Structures of monocyclic and bicyclic *N*-nitrosamines were optimized by means of density functional theory

(18) **Crystallographic data for bicyclic *N*-nitrosamine **2****: C<sub>18</sub>H<sub>13</sub>N<sub>3</sub>O<sub>3</sub>/1/2CH<sub>3</sub>OH,  $M_r = 335.34$ , 0.35 mm × 0.05 mm × 0.49 mm, triclinic  $P\bar{1}$ ,  $a = 11.5753(8)$  Å,  $b = 17.742(1)$  Å,  $c = 8.3025(8)$  Å,  $\alpha = 101.469(7)^\circ$ ,  $\beta = 102.858(7)^\circ$ ,  $\gamma = 90.456(6)^\circ$ ,  $V = 1626.7(2)$  Å<sup>3</sup>,  $Z = 4$ ,  $D_x = 1.369$  g/cm<sup>3</sup>,  $2\theta_{\max} = 135.2^\circ$ ,  $T = 296$  K,  $\mu(\text{Mo K}\alpha) = 8.02$  cm<sup>-1</sup>,  $F_{000} = 700$ , Rigaku RAXIS-II Imaging Plate diffractometer,  $\omega$  scans, 6109 refs measured, 5798 unique, 3516 with  $I > 3.0 \sigma(I)$ , 452 variables,  $R = 0.053$ ,  $R_w = 0.068$ ,  $S = 1.86$ ,  $(\Delta/\sigma)_{\max} = 0.14$ ,  $\rho\Delta_{\max} = 0.40$  eÅ<sup>-3</sup>,  $\Delta\rho_{\min} = -0.25$  eÅ<sup>-3</sup>.

(DFT) calculations (B3LYP/6-31G\*) (Figure 9).<sup>21</sup> Calculations included the experimentally studied monocyclic *N*-nitrosamines **12–17** and **19**.

Experimentally unstable *N*-nitrosoaziridine (**21**)<sup>22</sup> was also studied theoretically. The structure of **21** is consistent with the previous calculation.<sup>22</sup> Bicyclic *N*-nitrosamines included the

(19) **Crystallographic data for bicyclic *N*-nitrosamine **4****: C<sub>14</sub>H<sub>14</sub>N<sub>2</sub>O<sub>5</sub>,  $M_r = 290.27$ , 0.40 mm × 0.34 mm × 0.30 mm, monoclinic  $P2_1/a$ ,  $a = 9.187(9)$  Å,  $b = 11.559(9)$  Å,  $c = 13.164(4)$  Å,  $\beta = 102.20(4)^\circ$ ,  $V = 1366.46(0)$  Å<sup>3</sup>,  $Z = 4$ ,  $D_x = 1.411$  g/cm<sup>3</sup>,  $2\theta_{\max} = 41.7^\circ$ ,  $T = 296$  K,  $\mu(\text{Mo K}\alpha) = 0.00$  cm<sup>-1</sup>,  $F_{000} = 608$ , Rigaku RAXIS-II Imaging Plate diffractometer,  $\omega$  scans, 1332 refs measured, 1308 unique, 1267 with  $I > 2.0 \sigma(I)$ , 191 variables,  $R = 0.065$ ,  $R_w = 0.085$ ,  $S = 4.30$ ,  $(\Delta/\sigma)_{\max} = 0.094$ ,  $\rho\Delta_{\max} = 0.28$  eÅ<sup>-3</sup>,  $\Delta\rho_{\min} = -0.28$  eÅ<sup>-3</sup>.

(20) **Crystallographic data for bicyclic *N*-nitrosamine **10****: C<sub>10</sub>H<sub>14</sub>N<sub>2</sub>O<sub>5</sub>,  $M_r = 242.23$ , 0.50 mm × 0.30 mm × 0.30 mm, monoclinic  $P2_1/c$ ,  $a = 13.4601(8)$  Å,  $b = 7.3065(4)$  Å,  $c = 12.1746(7)$  Å,  $\beta = 110.8900(10)^\circ$ ,  $V = 1118.62(10)$  Å<sup>3</sup>,  $Z = 4$ ,  $D_x = 1.438$  g/cm<sup>3</sup>,  $2\theta_{\max} = 57.0^\circ$ ,  $T = 93$  K,  $\mu(\text{Mo K}\alpha) = 0.16$  cm<sup>-1</sup>,  $F_{000} = 512$ , Bruker SMART CCD diffractometer,  $\omega$  scans, 6740 refs measured, 2815 unique, 2164 with  $I > 3.0 \sigma(I)$ , 155 variables,  $R = 0.060$ ,  $R_w = 0.067$ ,  $S = 3.85$ ,  $(\Delta/\sigma)_{\max} = 4.45$ ,  $\rho\Delta_{\max} = 0.66$  eÅ<sup>-3</sup>,  $\Delta\rho_{\min} = -0.67$  eÅ<sup>-3</sup>.

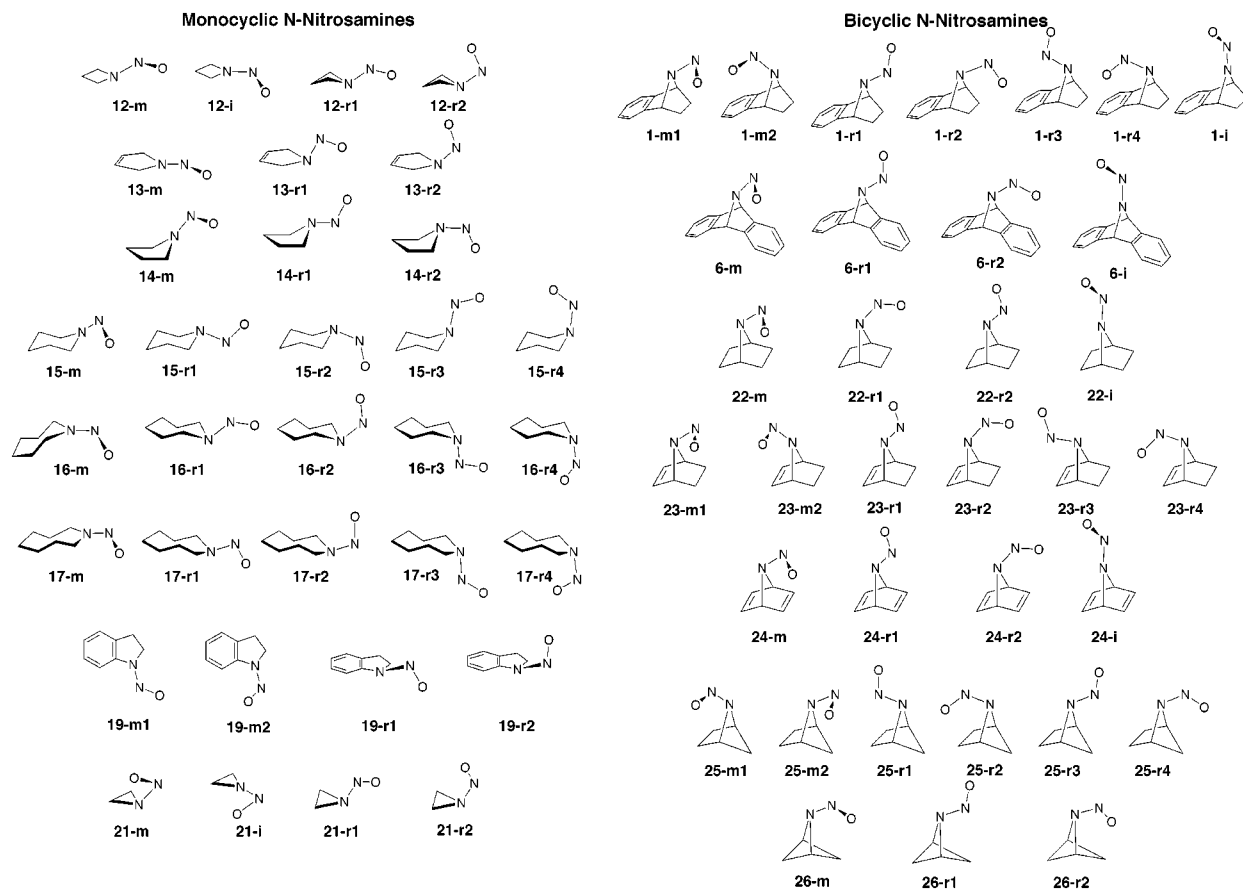


Figure 9. Optimized structures of N-nitrosamines.

parent N-nitrosamines of 7-azabicyclo[2.2.1]heptane (**22**), 7-azabicyclo[2.2.1]heptene (**23**), 7-azabicyclo[2.2.1]heptadiene (**24**), 7-azabenzobicyclo[2.2.1]heptane (**1**), and 7-azadibenzobicyclo[2.2.1]heptane (**6**). Nitrosamines of a different bicyclic system, N-nitroso-6-azabicyclo[2.1.1]hexane (**25**) and N-nitroso-5-azabicyclo[1.1.1]pentane (**26**), were also calculated to compare the structural features among the bicyclic systems.

**Geometries.** The energy minimum structures of the bicyclic N-nitrosamines of 7-azabicyclo[2.2.1]heptane (**1**, **6**, **22**, **23**, and **24**) were found to be nitrogen-pyramidal (**1-m1**, **1-m2**, **6-m**, **22-m**, **23-m1**, **23-m2**, and **24-m**), the  $\theta$  values being smaller than  $360^\circ$  (Figure 9 and Supporting Information, Table S1). Calculations reproduced the pyramidalized nitroso groups found in the crystal state (Figure 8). The corresponding nitrogen planar structures (**6-i**, **22-i**, and **24-i**) were transitional, the calculated inversion barriers being less than 1 kcal/mol (0.51, 0.78, and 0.48 kcal/mol, respectively (B3LYP/6-311G\*\*)) (Supporting Information, Table S2). The global minima of other bicyclic nitrosoamines **25m** and **26m** are also nitrogen-pyramidal (see

Table S1). The inversion barriers of **25m** and **26m** are relatively high (3.56 and 4.54 kcal/mol, respectively), suggesting that the pyramidal nitrogen structure is thermodynamically stable.

In the case of the unsymmetrical bicyclic nitrosamines (**1**, **23**, and **25**), two orientations of nitrogen pyramidalization are possible (see Table S3 in the Supporting Information). In the case of 7-azabenzobicyclo[2.2.1]heptane **1**, the structure (**1-m1**) in which the NO group is tilted on the side opposite from the benzene ring was more stable than the structure (**1-m2**) with the tilt of the NO group on the side of the benzene ring. While the energy difference was small (by 0.62 kcal/mol (B3LYP/6-311G\*\*)), this structural preference was consistent with the structures of two N-nitroso-7-azabenzobicyclo[2.2.1]heptane derivatives (**2** and **4**) found in the solid state (Figure 8). The nitrosamine **23** favored the structure (**23-m1**) in which the NO group is opposite to the double bond, the energy difference from **23-m2** being small (0.54 kcal/mol). The nitrosamines of a different bicyclic system, 6-azabicyclo[2.2.1]heptane (**25**) and 5-azabicyclo[1.1.1]pentane (**26**), also take pyramidal nitrogen structures (Figure 9 and Table S1). The nitrosamine **25** favored the invertmer **25-m1** over **25-m2** (Figure 9), the energy difference being 2.59 kcal/mol.

**Rotational Barriers.** Rotational barriers with respect to the N–NO bonds were calculated at the level of the B3LYP/6-311G\* basis set (Table 3). Two transitional rotational conformations of N-nitrosamines were calculated, *s-cis* (**r1**) and *s-trans* (**r2**) conformations (in which the NO bond is anti-periplanar or syn-periplanar with respect to the nitrogen lone pair) (Figure 9). In all cases studied here, the *s-cis* conformation was favored over the *s-trans* conformation (see Table S3 in the Supporting Information).<sup>24</sup> Rotational barriers about the N–NO bonds were evaluated on the basis of the most stable ground

(21) Frisch, M. J.; Trucks, G. W.; Schlegel, H. B.; Gill, P. M. W.; Johnson, B. G.; Robb, M. A.; Cheeseman, J. R.; Keith, T.; Petersson, G. A.; Montgomery, J. A.; Raghavachari, K.; Al-Laham, M. A.; Zakrzewski, V. G.; Ortiz, J. V.; Foresman, J. B.; Cioslowski, J.; Stefanov, B. B.; Nanayakkara, A.; Challacombe, M.; Peng, C. Y.; Ayala, P. Y.; Chen, W.; Wong, M. W.; Andres, J. L.; Replogle, E. S.; Gomperts, R.; Martin, R. L.; Fox, D. J.; Binkley, J. S.; Defrees, D. J.; Baker, J.; Stewart, J. P.; Head-Gordon, M.; Gonzalez, C.; Pople, J. A. *Gaussian 94*, revision D.3; Gaussian, Inc.: Pittsburgh, PA, 1995.

(22) N-Nitrosoaziridine is unstable at room temperature, which decomposes to ethylene and nitrous oxide (N<sub>2</sub>O). (a) Rundel, W.; Müller, E. *Chem. Ber.* **1963**, *96*, 2528–2531. (b) Clark, R. D.; Helmkamp, G. K. *J. Org. Chem.* **1964**, *29*, 1316–1320. (c) Shustov, G. V.; Kachanov, A. V.; Kadorkina, G. K.; Kostyanovsky, R. G.; Rauk, A. *J. Am. Chem. Soc.* **1992**, *114*, 8257–8262. (d) Shustov, G. V.; Rauk, A. *J. Am. Chem. Soc.* **1995**, *117*, 928–934.

**Table 3.** Calculated Rotational Barriers (kcal/mol) of N–NO Bonds

	A:6-31G* B: 6-311G**					
	HF/A	B3LYP/A	B3LYP/B	corrected <sup>a</sup>	CCSD(T)/A <sup>b</sup>	corrected <sup>c</sup>
Bicyclic Nitrosamines						
<b>1m1</b> → <b>1r1</b>	15.77	19.90	19.70	19.26 <sup>d</sup>	—	—
<b>6m</b> → <b>6r1</b>	15.40	19.04	18.84	18.28	—	—
<b>22m</b> → <b>22r1</b>	15.21	19.46	19.17	18.76	15.36	14.95
<b>23m1</b> → <b>23r1</b>	15.68	19.99	19.66	19.21 <sup>e</sup>	15.82	15.37
<b>24m</b> → <b>24r1</b>	15.38	19.34	19.22	18.65	14.93	14.36
<b>25m1</b> → <b>25r1</b>	14.07	17.39	17.23	16.78 <sup>f</sup>	14.16	13.71
<b>26m</b> → <b>26r1</b>	10.23	13.11	13.02	12.65	10.12	9.75
Monocyclic Nitrosamines						
<b>12m</b> → <b>12r1</b>	7.92	21.59	21.23	20.77	17.09	16.63
<b>13m</b> → <b>13r1</b>	21.31	25.15	24.65	24.00	21.15	20.50
<b>14m</b> → <b>14r1</b>	21.31	25.15	24.76	23.60	21.45	20.29
<b>15m</b> → <b>15r1</b>	19.39	25.07	24.48	23.96	20.51	19.99
<b>16m</b> → <b>16r1</b>	23.61	28.49	27.89	27.16	24.36	23.63
<b>17m</b> → <b>17r1</b>	22.19	27.76	27.13	26.42	23.32	22.61
<b>19m1</b> → <b>19r1</b>	20.95	24.44	23.81	23.27 <sup>g</sup>	—	—
<b>21m</b> → <b>21r1</b>	3.99	6.03	5.58	5.21	3.51	3.06

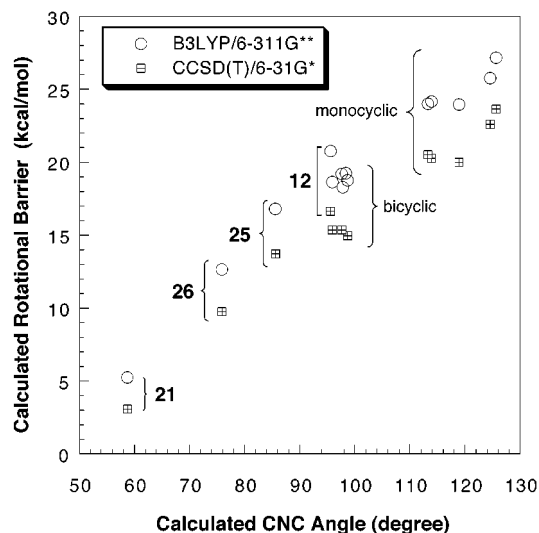
<sup>a</sup> B3LYP/B values, corrected with scaled zero-point energy based on HF/6-31G\* frequency calculations (scaled by 0.89). <sup>b</sup> Frozen-core approximation. <sup>c</sup> CCSD(T)/A values, corrected similarly as in *a*. <sup>d</sup> **1m2**→**1r3**: 17.85 kcal/mol (B3LYP/B, corrected). <sup>e</sup> **23m2**→**23r3**: 18.01 kcal/mol (B3LYP/B, corrected). <sup>f</sup> **25m2**→**25r3**: 16.04 kcal/mol (B3LYP/B, corrected). <sup>g</sup> **19m2**→**19r2**: 20.55 kcal/mol (B3LYP/B, corrected).

minimum structures of the nitrosamines, and the values are shown in Table 3. The rotational barriers (except **1**, **6**, and **19**) were also evaluated with a coupled cluster method, CCSD(T)/6-31G\* which represents a more accurate treatment of electron correlation. The relative orders of magnitude of the computed rotational barriers obtained at both calculation levels (DFT and CCSD(T)) are consistent with those of the experimental  $\Delta G_c^\ddagger$  values obtained in solution (Table 1). The calculated values are consistently larger (in the case of B3LYP/6-311G\*\*) and smaller (in the case of CCSD(T)/6-31G\*) than the experimental values. The rotational barriers of the monocyclic *N*-nitrosamines (**12**–**17**) can be estimated computationally. The calculations at both DFT and CCSD(T) levels suggested that the computed rotational barriers of the bicyclic nitrosamines of 7-azabicyclo[2.2.1]heptanes (**1**, **6**, **22**, **23**, and **24**) are generally smaller than those of the monocyclic ones (**13**–**17**) (an apparent exception is *N*-nitrosoaziridine **12**) (Table 3, see also Figure 10). This conclusion is valid even when the rotational barriers derived from the less stable conformers of the *N*-nitrosamines (that is, **1-m2**, **23-m2**, and **25-m2**) are considered (see Table 3 footnote). The rotational barrier of the *N*-nitrosoindoline **19**, experimentally inaccessible, was evaluated computationally to be 23.3 kcal/mol (B3LYP/6-311G\*\*), the value being comparable with the barriers of monocyclic nitrosamines. The nitrosamines of different bicyclic systems, **25** and **26**, have rotational barriers smaller than those of the nitrosamines of 7-azabicyclo[2.2.1]-heptanes (Table 3).

A bicyclic 7-azabicyclo[2.2.1]heptane motif can impose angle strain on the nitrogen atom of the pyrrolidine ring due to the ethano bridge.<sup>6</sup> The optimized CNC angles of the bicyclic nitrosamines (**1**, **6**, **22**–**24**) are smaller than those of the monocyclic ones (except the small-ring analogues **12** and **21**) (see Table S1). In fact, the CNC angle at the bridgehead nitrogen atom of *N*-nitrosamines of 7-azabicyclo[2.2.1]heptanes **2**, **4**, and **10** is decreased to 99°, smaller than that of **13** (115°) in the

(23) Harris, N.; Lammertsma, K. *J. Am. Chem. Soc.* **1997**, *119*, 6583–6589.

(24) This conformational preference can be interpreted in terms of repulsive interactions of the vicinal nitrogen lone pair electrons of the amine and NO group in the *s-trans* rotated conformation.

**Figure 10.** Relationship between the CNC angle and rotational barrier. Becke3LYP/6-311G\*\* and CCSD(T)/6-31G\* Levels.

crystal structures. Replacement of the ethano bridge of the *N*-nitroso-7-azabicyclo[2.2.1]heptane with a methane bridge can increase angle strain upon the nitrosamine nitrogen atoms. Calculated structures of *N*-nitroso-6-azabicyclo[2.1.1]hexane **25** and *N*-nitroso-5-azabicyclo[1.1.1]pentane **26** have smaller CNC angles as compared with that of *N*-nitroso-7-azabicyclo[2.2.1]-heptane **22** (Table S1).

The computed rotational barriers apparently correlate with the computed CNC angles (Figure 10).<sup>25</sup> This indicates that the low rotational barriers of the N–NO bond of the aliphatic *N*-nitrosamines are due to angle strain of the amino nitrogen atom.

**Bond Model.** Rotational barriers of the N–NO bond reflect the magnitude of the *N*-nitroso resonance or the delocalization of the lone pair on the nitrogen atom to the N=O bond. The analysis of the electronic wave function at the RHF/6-31G\*\*/B3LYP/6-31G\* level according to the bond model method<sup>7,26,27</sup> showed that the delocalization index ( $|C_T/C_G|$ ) (Supporting Information, Table S4) for  $n_N$  to  $\sigma_{NO}^*$  correlated well with the computed rotational barriers of the *N*-nitrosamines (monocyclic **12**, **14**, and **21**; bicyclic **22**) (Figure 11).<sup>28</sup>

**Bond Strength.** Computed homolytic bond dissociation energy (BDE) is a theoretical index of bond strength. These values were estimated on the basis of B3LYP/6-311G\*\* and CCSD(T)/6-31G\* (except **1**, **6**, and **19**) basis sets (Table 4). The relative order of magnitudes of the BDE values are consistent within each of the calculation levels, DFT and

(25) Regression coefficients (*r*) were estimated to be 0.980 (B3LYP/6-311G\*\*) and 0.984 (CCSD(T)/6-31G\*), respectively.

(26) The single Slater determinant of the Hartree–Fock wave function ( $\Psi$ ) for the electronic structure of a molecule is expanded into electron configurations:<sup>8</sup>  $\Psi = C_G\Phi_G + \sum C_T\Phi_T + \dots$  In the ground configuration ( $\Phi_G$ ), a pair of electrons occupies each bonding orbital of the bonds. Electron delocalization is expressed by mixing an electron-transferred configuration ( $\Phi_T$ ), where an electron shifts from the bonding orbital of a bond to the antibonding orbital of another. A set of bond (bonding and antibonding) orbitals gives the coefficients of the electron configurations, i.e.,  $C_G$  and  $C_T$  values, and is optimized<sup>8</sup> to give the maximum value of the coefficient of the ground configuration. The delocalization index is defined as the relative ratio of the coefficient of the transferred configuration to that of the ground configuration ( $|C_T/C_G|$ ),<sup>27</sup> to show the delocalizability between the bonds.

(27) (a) Inagaki, S.; Kawata, H.; Hirabayashi, Y. *Bull. Chem. Soc. Jpn.* **1982**, *55*, 3724–3732. (b) Inagaki, S.; Goto, N.; Yoshikawa, K. *J. Am. Chem. Soc.* **1991**, *113*, 7144–7146. (c) Inagaki, S.; Yoshikawa, K.; Hayano, Y. *J. Am. Chem. Soc.* **1993**, *115*, 3706–3709. (d) Inagaki, S.; Ishitani, Y.; Kakefu, T. *J. Am. Chem. Soc.* **1994**, *116*, 5954–5958.

(28) A regression coefficient (*r*) was 0.999.

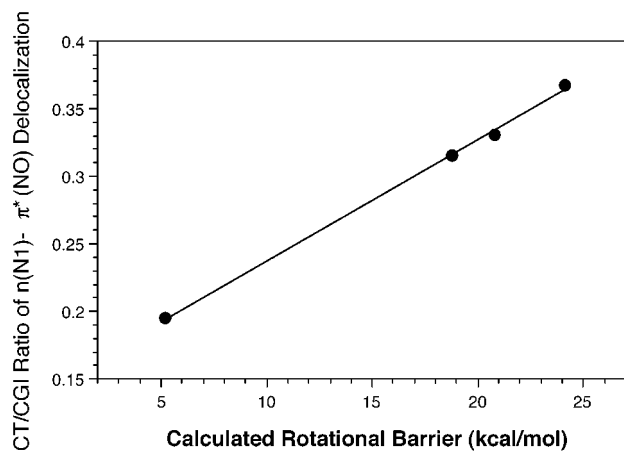


**Figure 11.** Relationship between electron delocalization and rotational barrier.

**Table 4.** Calculated Homolytic BDE of N–NO Bonds of N-Nitrosamines

	A:6-31G* B: 6-311G**		Corrected <sup>a</sup>	CCSD(T)/A <sup>b</sup>	Corrected <sup>c</sup>
	B3LYP/A	B3LYP/B			
Bicyclic Nitrosamines					
<b>1-m1</b>	40.09	38.89	35.34 <sup>d</sup>	—	—
<b>6-m</b>	36.87	35.58	32.21	—	—
<b>22-m</b>	41.95	40.56	36.81	39.96	36.21
<b>23-m1</b>	40.02	38.70	35.03 <sup>e</sup>	37.99	34.32
<b>24-m</b>	34.86	33.57	30.24	32.89	29.56
<b>25-m1</b>	39.26	37.98	34.15 <sup>f</sup>	37.38	33.55
<b>26-m</b>	31.06	29.79	26.13	28.40	24.74
Monocyclic Nitrosamines					
<b>12-m</b>	46.32	44.84	40.47	42.55	38.18
<b>13-m</b>	44.27	42.78	38.56	41.31	37.09
<b>14-m</b>	45.20	43.72	39.39	42.63	38.30
<b>15-m</b>	47.85	46.57	42.49	45.18	41.10
<b>16-m</b>	49.25	47.83	43.59	47.20	42.96
<b>17-m</b>	49.22	48.01	43.92	47.16	43.07
<b>19-m1</b>	34.03	32.72	27.59 <sup>g</sup>	—	—
<b>21-m</b>	33.40	31.89	27.72	30.27	26.10

<sup>a, b, c</sup> See the captions of Table 3. <sup>d</sup> **1m2**: 34.72 kcal/mol (B3LYP/B, corrected). <sup>e</sup> **23m2**: 34.45 kcal/mol (B3LYP/B, corrected). <sup>f</sup> **25m2**: 31.56 kcal/mol (B3LYP/B, corrected). <sup>g</sup> **19m2**: 24.87 kcal/mol (B3LYP/B, corrected).

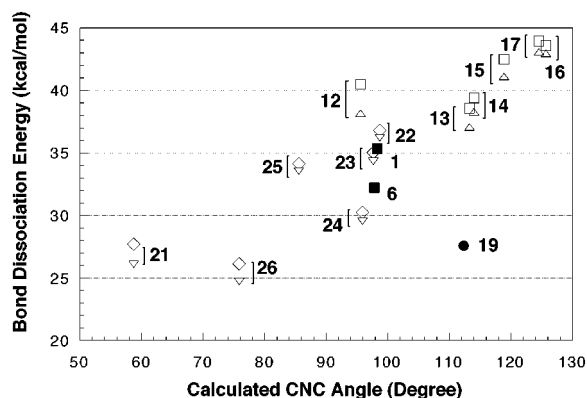


**Figure 12.** Relationship between the CNC angle and bond dissociation energy of alliphatic N-nitrosamines. Becke3LYP/6-311G\*\* (□, ■, ◇, ●) and CCSD(T)/6-31G\* (△, ▽) Levels. □, △ Negative Griess assay. ■ Positive and weakly positive Griess assay. ◇, ▽ Not examined experimentally. ● (**19**) Aromatic N-nitrosamine. Positive Griess assay.

CCSD(T) (see also Figure 12). The DFT and CCSD(T) calculations both suggested that the BDE values of the bicyclic N-nitrosamines of 7-azabicyclo[2.2.1]heptanes (**1**, **6**, **22**, **23**, and **24**) are generally smaller than those of monocyclic

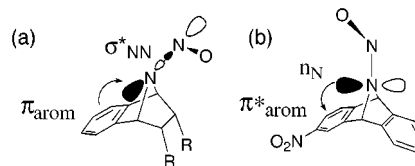


**Figure 13.** Anchimeric electron delocalization due to neighboring aromatic  $\pi$  orbitals.

N-nitrosamines (**12**, **13**, **14**, **15**, **16**, and **17**) (Table 4 and see also Figure 12). The exception is N-nitrosoaziridine **21**. The BDE value of N-nitrosoaziridine (**21-m**) is the smallest among the monocyclic N-nitrosamines. This result is consistent when the less stable conformational isomers of **1**, **19**, **23**, and **25** are considered (see Table 4 footnote). The aromatic N-nitrosamine, N-nitrosoindoline **19** (**19-m1**), also has a small BDE (27.6 kcal/mol, B3LYP/6-311G\*\*, Table 4), close to that of N-nitrosoaziridine **21-m** (27.7 kcal/mol, B3LYP/6-311G\*\*). These BDE data (Table 4) are consistent with the results of the Griess assay (Figure 4) which reflects the ease of N–NO bond cleavage. Furthermore, the BDE value of N-nitroso-5-azabicyclo[1.1.1]pentane **26** is comparable to that of N-nitrosoaziridine **21-m**, suggesting that N–NO bond cleavage is facilitated in **26**. The calculated CNC angle and computed BDE showed some correlation, but the plots are scattered, especially the value for **12** (Figure 12): N-nitrosoazetidine **12** has a high BDE despite its small CNC angle. The reason for the anomalous character of N-nitrosoazetidine **12** is not clear at present. The BDE value of N-nitrosoazetidine (**12-m**) is comparable to those of five- to eight-membered N-nitrosamines (**13-m**, **14-m**, **15-m**, **16-m**, and **17-m**). This is consistent with the observation that **12** is negative in the Griess assay.

In a series of N-nitrosamines of 7-azabicyclo[2.2.1]heptanes, introduction of a double bond decreases the BDE values (**22** → **23** → **24**) (Table 4 and Figure 12) while the CNC angle is decreased in the same order (Table S1). Thus, we postulate that the reduction of the resonance in the N–NO group of the bicyclic derivatives (**1**–**11**) is important for promoting N–NO bond cleavage. Electron delocalization arising from the interaction of the aromatic  $\pi$  orbital with the vacant antibonding  $\sigma^*_{N-N}$  orbital (Figure 13a), or from the interaction of the nitrogen nonbonding orbital with the vacant aromatic  $\pi^*$  orbital (Figure 13b) can weaken the N–NO bond (Figure 13). Such interactions would account for the facile bond cleavage of **2**, **3**, **4**, **5**, **7**, **8**, and **9**, which bear a benzo group or withdrawing substituents.

In conclusion, the N–NO bond of aliphatic N-nitroso derivatives of 7-azabicyclo[2.2.1]heptanes tends to be weak, probably due to angle strain. This is reflected in reduced rotational barriers of the N–NO bonds in solution and nitrogen-pyramidal structures of the N-nitroso group in the solid state. The present computations predict that N–NO bond cleavage is also facilitated in N-nitroso derivatives (**26**) of 5-azabicyclo[1.1.1]pentane, although the parent bicyclic amine (5-azabicyclo[1.1.1]pentane) is of only theoretical interest at present.<sup>29</sup> The present work has established the structural features of aliphatic N-nitrosamines that facilitate N–NO bond cleavage, and the results indicate that certain aliphatic N-nitrosamines may act as efficient donors of NO-related species.

**Acknowledgment.** This work was supported partly by Grants-in-Aid from the Ministry of Education, Science, Sports

(29) (a) Ebrahimi, A.; Deyhimi, F.; Roohi, H. *J. Chem. Res., Synop.* **2000**, 2, 93–95. (b) Belostotskii, A. M.; Aped, P.; Hassner, A. *THEOCHEM* **1998**, 429, 265–273. (c) Belostotskii, A. M.; Aped, P.; Hassner, A. *THEOCHEM* **1997**, 398–399, 427–434.



and Culture, Japan for Scientific Research. We thank Professor Dr. Kimihiko Hirao, Department of Applied Chemistry, Graduate School of Engineering, the University of Tokyo for the help and discussion in the computational study. T.O. also thanks the Computer Center of the University of Tokyo for generous allotment of computer time.

**Supporting Information Available:** Full experimental detail, computational detail (Tables S1–S4), and supplementary figures (Figures S1 and S2) (PDF). This material is available free of charge via the Internet at <http://pubs.acs.org>.

JA010917D